



HAL
open science

DMD algorithms for experimental data processing in combustion

Franck Richecoeur, Loyal Hakim, Antoine Renaud, Laurent Zimmer

► **To cite this version:**

Franck Richecoeur, Loyal Hakim, Antoine Renaud, Laurent Zimmer. DMD algorithms for experimental data processing in combustion. Proceeding of the 2012 Summer Program, Center for Turbulence Research, Stanford University, pp.459-468, 2012. hal-00825509

HAL Id: hal-00825509

<https://hal.science/hal-00825509v1>

Submitted on 23 May 2013

HAL is a multi-disciplinary open access archive for the deposit and dissemination of scientific research documents, whether they are published or not. The documents may come from teaching and research institutions in France or abroad, or from public or private research centers.

L'archive ouverte pluridisciplinaire **HAL**, est destinée au dépôt et à la diffusion de documents scientifiques de niveau recherche, publiés ou non, émanant des établissements d'enseignement et de recherche français ou étrangers, des laboratoires publics ou privés.

DMD algorithms for experimental data processing in combustion

By F. Richecoeur^{†‡}, L. Hakim^{†‡}, A. Renaud^{†‡} AND L. Zimmer^{†‡}

The present study aims at investigating the parameters influencing the quality of the dynamic mode decomposition when applied to experimental data from turbulent combustion. It is shown that the choice of the snapshots and the decomposition methodology have a strong influence on the mode spectra and the frequency resolution. Finally, the simultaneous decomposition of experimental data is performed with optimal parameters showing the quantitative information which can be obtained to highlight the coupling mechanisms involved in combustion instabilities.

1. Introduction

Combustion instabilities result from a powerful coupling between turbulence, combustion and acoustics leading to damaging pressure oscillations in industrial furnaces, gas turbines or aeronautic turbines (Candel *et al.* 2009). To better understand the underlying mechanisms, experiments have been designed to mimic real configurations featuring thermo-acoustic instabilities (Huang & Yang 2009) and were equipped with high performance diagnostics allowing to track heat release rate, flame front, velocity fields, acoustics, spray distribution with the highest possible resolution both in space and time (Ballester & Garcia-Armingol 2010; Aldén *et al.* 2011; Schulz & Sick 2005). It is now understood that instabilities emerge from a resonant coupling between acoustics, combustion and aerodynamics. To highlight these phenomena, diagnostics require post-processing to correlate physical quantities and extract complementary information.

Commonly used post-processing tools, such as Fourier transforms, Fast Fourier Transforms (FFT), phase averaging, cross-correlation, wavelets, λ_2 criterion. . . , can be applied to describe combustion dynamics. All these processing techniques aim at filtering or projecting the data to extract coherent components from turbulent quantities. Recently *Proper Orthogonal Decomposition* (Berkooz *et al.* 1993) emerged as a decomposition tool in most energetic orthogonal modes. This technique has been extensively used to analyze velocity fields in unsteady flows (Gilliam *et al.* 2004) and in combustion chambers (Stöhr *et al.* 2011; Duwig *et al.* 2012). The first advantage of POD is that it can be used with non time-resolved data. The second advantage of this tool is its ability to compute modes from the data snapshots without preconceived knowledge of the flow dynamics. The third advantage of POD is the possibility to correlate diagnostics by using extended-POD (Glezer *et al.* 1989; Maurel *et al.* 2001; Borée 2003; Duwig & Iudiciani 2010) where information from two different quantities can be merged to extract dynamics and interactions. This interesting processing creates an orthogonal projection basis from one diagnostics then another diagnostics is projected on it so that the main modes are the one featuring a strong correlation between the different quantities. However, POD suffers

[†] CNRS, Laboratory EM2C UPR 288, Grande Voie des Vignes, F-92295 Châtenay-Malabry

[‡] École Centrale Paris, Grande Voie des Vignes, F-92295 Châtenay-Malabry

from limitations due to the lack of criteria to choose the dynamically active modes and provides limited interpretation since the time component is generally not resolved.

Dynamic Mode Decomposition (DMD) is one of the most recent post-processing tool taking advantage of the richness in space and time of the current diagnostics (Schmid 2010; Schmid *et al.* 2011). The dynamic decomposition is based on the Koopman modes (Rowley *et al.* 2009) to extract modes from the data snapshots and to associate an unique frequency to each mode. This is of major interest for combustion applications where one wants to be able to separate phenomena occurring at different frequencies. Similarities between POD and DMD have been highlighted by Muld *et al.* (2012), Schmid *et al.* (2012) and Semeraro *et al.* (2012) showing that DMD modes may be reconstructed from POD modes. However, to extract information from the time resolved data gathered with multi-diagnostics in combustion chambers, DMD seems to be an appropriate candidate given its easiness of implementation and its low CPU cost. DMD was essentially applied to velocity fields and nothing has been performed in reactive flows. Especially in two-phase combustion, data concerning the liquid distribution, acoustics and heat release may be exploited to investigate the combustion dynamics. Such systems show non-linear couplings that are very complicated to describe with the traditional post-processing tools. The purpose of this research is to investigate the benefits of using DMD to analyze combustion dynamics and investigate the bias of the methodology when dealing with experimental data.

In literature, different computing algorithms have been presented leading to different ways of computing spectra. The first section of the report analyzes the two main algorithms, points the link between them and proposes different ways of simultaneously analyze different diagnostics to highlight correlations. The second section presents the different bias observed on the processing of two-phase flow measurements and some ideas to adapt and improve the processing technique for experimental combustion. In the third part, the two DMD computing techniques are tested on experimental measurements obtained in a turbulent combustion chamber.

2. Methodology

In this section two different methods are detailed. The first one is called “multiple-variable” DMD and gives an optimal basis for all the diagnostics. The second one, the “extended” DMD is developed in the manner of extended POD from Borée (2003) and gives information on diagnostics correlation.

2.1. DMD calculation

DMD of the experimental data is obtained as introduced by Schmid (2010) and exemplified in Schmid (2011) and Schmid *et al.* (2012). Let (v_i) , $i \in \llbracket 1, N + 1 \rrbracket$, be $N + 1$ vectors representing $N + 1$ experimental snapshots (of velocity or radical OH* fields for example) equally spaced in time. A matrix $V_1 = (v_1, v_2, \dots, v_N)$ is formed with the N first vectors. The main idea of DMD is to assume the existence of a constant linear mapping A relating v_i to the subsequent v_{i+1} , such that one may write V_1 as a Krylov space

$$V_1 = \{v_1, Av_1, \dots, A^{N-1}v_1\}$$

If the sequence is sufficiently long (N sufficiently large), the vectors $(v_i)_{i \in \llbracket 1, N+1 \rrbracket}$ become linearly dependent. The vector v_{N+1} is then expressed as a linear combination of the

independent sequence $(v_i)_{i \in [1, N]}$:

$$V_2 = (v_2, v_3, \dots, v_{N+1}) = AV_1 = V_1 S + \mathbf{r} \quad (2.1)$$

where \mathbf{r} is the residual vector. The eigenvalues of S then approximate the eigenvalues of A . The objective is to minimize the residual:

$$S = \arg \min_S \|V_2 - V_1 S\|$$

First a singular value decomposition of V_1 is used:

$$V_1 = U \Sigma W^H \quad (2.2)$$

where U contains the proper orthogonal modes of V_1 , Σ is a square diagonal matrix containing the singular values of V_1 , and W^H is the conjugate transpose of W , the right-singular matrix of V_1 for the singular values Σ . S is calculated by multiplying V_2 by the V_1 pseudoinverse:

$$S = V_1^+ V_2 = W \Sigma^{-1} U^H V_2 = Y' \Lambda (Y')^{-1}$$

with Y' and Λ the eigenvectors and eigenvalues of S . Thus the projection of V_2 on the modes $V_1 Y'$ gives:

$$V_2 = (V_1 Y') \Lambda (Y')^{-1} \quad (2.3)$$

From this expression, one obtains the contribution of each dynamic mode to the data sequence V_2 :

- its amplitude is given by the norm of the corresponding column vector of $V_1 Y'$,
- its frequency and damping are provided by the eigenvalues in Λ .

Another way of proceeding is to use the V_1 decomposition of Eq. (2.2) and replace in Eq. (2.1). Rearranging terms, one obtains:

$$U^H V_2 W \Sigma^{-1} = U^H A U = \tilde{S} = Y \Lambda Y^{-1} \quad (2.4)$$

so that the eigenvalues Λ and eigenvectors Y of \tilde{S} are directly linked to those of A and the eigenvalues and eigenvectors of A are given by Λ and UY , respectively. One can note that S and \tilde{S} are similar, thus, they have the same eigenvalues:

$$S = W \Sigma^{-1} \tilde{S} (W \Sigma^{-1})^{-1} \quad (2.5)$$

Now V_2 may be projected onto a basis formed by the eigenmodes UY of A . One gets:

$$V_2 = (UY) \Lambda Y^{-1} \Sigma W^H \quad (2.6)$$

From this expression, one retrieves the contribution of each dynamic mode to the data sequence V_2 :

- its amplitude is given by the norm of the corresponding line vector in $Y^{-1} \Sigma W^H$,
- its frequency and damping are provided by the eigenvalues in Λ .

2.2. Multi-variable DMD

In this method, the data matrix V_1 is composed of a superposition of different variables (pressure, velocity, ...) placed one after the other as illustrated in Figure 1.

A DMD on V_1 results in a basis of dynamic modes which is common to all the variables. Thus, it describes the whole system dynamics and not only one variable dynamics.

The problem is that the amplitude of each dynamic mode does not give information

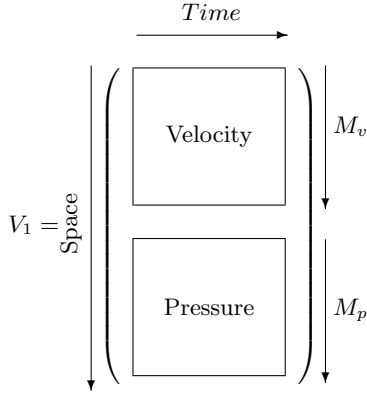


FIGURE 1. Data matrix in the multi-variable DMD. M_v is the space length for velocity diagnostics and M_p is the space length for pressure diagnostics.

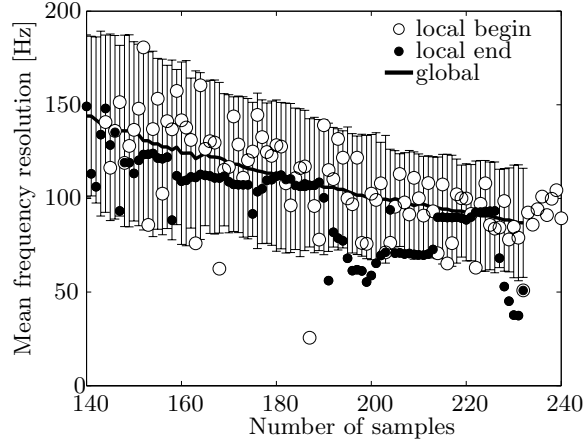


FIGURE 2. Effects of the number of samples on the mean, fluctuating and local spectral resolution. *Local begin* corresponds to a fixed initial snapshot whereas *local end* corresponds to a fixed final snapshot for the frequency resolution around the PVC frequency.

on the respective contribution of each variable to this mode. The idea is then to plot one spectrum for each variable instead of one spectrum for all the variables. In the example depicted in Fig. 1, the peak amplitude A_k at each eigenfrequency ω_k is calculated for the velocity spectrum by:

$$A_k = \|UY(1 : M_v, k)\| \times \|Y^{-1}\Sigma W^H(k, :)\| \quad (2.7)$$

and for the pressure spectrum by: $A_k = \|UY(M_v + 1 : M_v + M_p, k)\| \times \|Y^{-1}\Sigma W^H(k, :)\|$. With these two expressions, the contribution of each variable to the system dynamics can be quantified. The same methodology can be developed from equation (2.3).

2.3. Extended DMD

Another way to analyze the dynamics of a system with multiple diagnostics is to compute an "extended" DMD. The idea, derived from extended POD (Borée 2003), is to compute a frequency basis from one diagnostics and to make the projection of the second diagnostics onto this basis.

Let now $V_1 = (v_1, v_2, \dots, v_N)$ be a data matrix of N velocity snapshots and $P_1 = (p_1, p_2, \dots, p_N)$ a data matrix of pressure signals sampled at the same instants as the velocity snapshots. As explained in Section 2.1, a DMD on pressure gives:

$$P_2 = U_p Y_p \Lambda_p Y_p^{-1} \Sigma_p W_p^H \quad (2.8)$$

The columns of $\phi = U_p Y_p$ are the pressure spatial modes. Their amplitude and temporal evolution are contained in $B = \Lambda_p Y_p^{-1} \Sigma_p W_p^H$. We look for the velocity spatial modes ψ that have the same time evolution than the pressure spatial modes. Thus, ψ must satisfy: $V_2 = \psi B'$, where the elements of B' are defined as follows:

$$B'(i, j) = \frac{B(i, j)}{\|B(i, :)\|}, \quad (i, j) \in \llbracket 1, N \rrbracket^2 \quad (2.9)$$

In other words, the lines of B are normalized so that the amplitude A_k of each spatial mode corresponding to the eigenfrequency ω_k in B' can be retrieved by:

$$A_k = \|\psi(:, k)\| \quad (2.10)$$

The extended DMD does not provide a common basis to all the variables but an optimized basis for one selected diagnostics. One can then quantify what portion of a given diagnostics dynamics occurs at a given frequency. This portion is obtained as a ratio to the mean value. The common basis B can be computed from one diagnostics or the other, and with one of the two decompositions in equations (2.3) or (2.6).

3. Observations on DMD computations

In practical cases, several problems have to be solved when applying DMD algorithms. One has to choose the number of snapshots to deal with but also the most appropriate series of snapshots from the experiments, knowing that some of the data may contain noisy information. In this section, we report some key phenomena observed on DMD computation of experimental data: (1) the frequency resolution depending on the number of snapshots, (2) the influence of the last snapshot of the series and (3) the positive effect of computing simultaneously several diagnostics with the multi-variable DMD.

3.1. Frequency resolution and last snapshot dependency

One of the important aspects with DMD is that the spectral resolution may be variable. It is known that applying DMD algorithms on fluctuating data (removing the mean) will lead to a uniform frequency base, similar to the one obtained by Fourier transform as shown by Chen *et al.* (2012). On the other hand, making the decomposition on the raw data (without subtracting the mean) will lead to a non uniform frequency content. To illustrate the influence of the number of snapshots on the frequency resolution, data gathered on a multi-point injector are used (see Providakis *et al.* (2012) for more details of the configuration). DMD is applied on the Mie scattering of dodecane droplets conveyed by a swirled flow and recorded in a cross-plane of the combustion chamber, 15 mm from the exit of the injector at a frequency of 10 kHz. The data are simply resized so as to keep values in a matrix of 115×115 pixel. This flow presents a Precessing Vortex Core type of instability around 2500 Hz. The mean frequency resolution follows the classic decrease with an increase of the number of samples (see the continuous line in figure 2). On the same plot, the standard deviation of the frequency resolution is also given. This deviation is due to the variation of the resolution frequency depending on the frequency for a given series. One can see that variations around the mean frequency resolution is very important as one may have ± 40 Hz for a mean resolution of 142 Hz. This mean fluctuation tends to decrease with an increase in the number of samples, however, its relative level stays quite constant.

But the most important information is the local frequency resolution around the frequency of interest (here the PVC frequency). It is known that this local frequency may depend both on the number of snapshots and on the last snapshot, especially when using experimental data (Chen *et al.* 2012). In figure 2, the local frequency resolution around 2500 Hz is represented with dots. For a given number of snapshots, we can either fix the initial snapshot (white dots) or fix the last snapshot (black dots) of the series. This way, we can observe simultaneously the variations of the frequency resolution with the number of snapshots and the last snapshot. When the last snapshot is kept constant (black dots), the frequency resolution decreases like the mean evolution even if a large

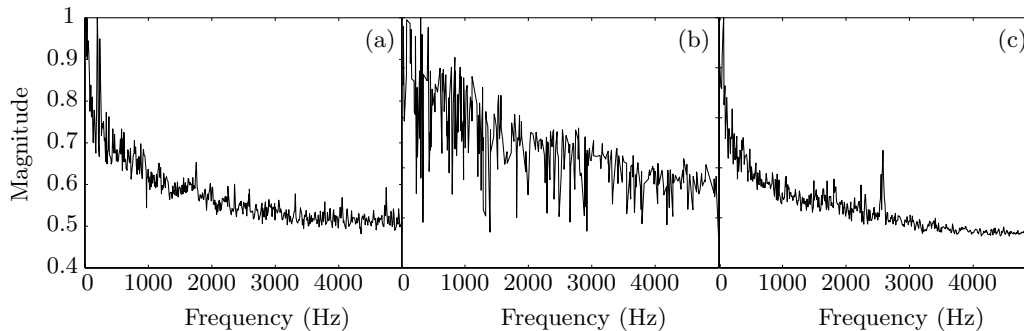


FIGURE 3. DMD spectra of (a) velocity, (b) Mie scattering, (c) Mie scattering and PIV field.

dispersion may be observed for some frequency ranges. When the initial snapshot is kept constant and the last one is changed, the fluctuation of the frequency resolution may be stiff. One can see interesting features for some case for which the frequency resolution is much smaller than the average, which may represent a good DMD mode, with a strong and well defined peak. Therefore, if one wants to have an optimal DMD, it seems better to have a fixed starting snapshot and to change the last snapshot until the frequency resolution shows a specific decrease. The quality of the last snapshot strongly influences the quality of the DMD, the number of snapshots is not the only parameter to play with to achieve an optimal resolution. Unfortunately, no rules can be deduced for an appropriate choice of snapshot series and frequency resolution and residuals should be checked for every computation.

Finally, another way to improve the detection of coherent structures may be to combine data. To illustrate this process, one uses the multi-variable DMD algorithm (Eq.2.6) and combine both PIV velocity field and Mie scattering data. For this example, 1000 samples are used on both the velocity field and Mie scattering. First, two decompositions are computed on separated variables. One can see that the spectra obtained for PIV alone does not exhibit a strong peak around 2500 Hz (Fig. 3(a)). The same observation is also done on Mie scattering data (Fig. 3(b)). The DMD spectrum is much noisier than in PIV case. Interestingly, when applying multi-variable DMD with the same data, one can see the peak around 2500 Hz becoming clear. It may be shown also that there exists an optimum to adjust the scales of the different variables. In the present case, the optimum for fast convergence of the DMD was obtained for a PIV velocity field with values ranging from -10 m/s to +50 m/s whereas Mie scattering data was ranging from 0 to 36000 counts. For a different scaling of the data, while analyzing the same snapshots, the structure could not be recovered. However, this optimum will depend on the actual variables, so no general rules may be obtained.

We consider these observations are extremely important. They emerge from the analysis of experimental data and prove that DMD computation has to be run with care to deal with the irregular quality of the experimental snapshots.

3.2. Discussion

As it is emphasized, one of the main drawbacks of the DMD technique when it comes to dealing with experimental data is its dependency to the last snapshot. A method, which can be viewed as an extension of the extended DMD technique, is presented here as a work in progress and no example will be given. Its objective is to help counter this phenomenon and to improve signal to noise ratio. It is inspired by the averaged

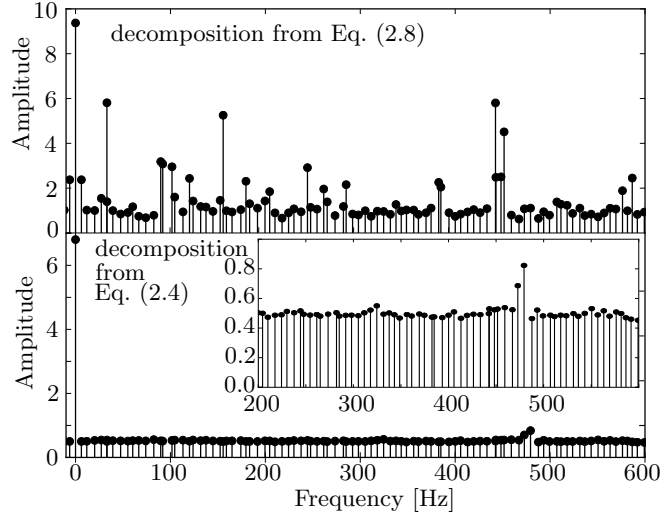


FIGURE 4. The spectra of the two decompositions from Eq.(2.4) and (2.8) are compared. The eigenfrequencies and the damping are the same but the mode amplitudes change drastically.

periodogram method commonly used in Fourier analysis. The leading idea is to divide the snapshot sequence into n successive and separate blocks of the same length $\{V^1, \dots, V^n\}$, to apply the extended DMD technique to these blocks as if they were different data sets and then to average the resulting modes for each relevant frequency. The periodogram method can be directly applied for Fourier transform since the decomposition basis is predetermined. On the contrary, the key feature of the DMD is its capability to extract an adequate basis from the data. A first step is therefore to obtain a common basis on which to project each part. This is done by performing a DMD analysis on one of these blocks to get the basis and the modes for this part: $V_j = \Phi_j B$. The projection of the other parts on the basis B is then performed: $\Phi_i = V_i B^{-1}$. Only one DMD is indeed performed, the other steps just being projections of the data on the previously computed basis.

The spectrum is obtained by plotting the average of the norms of the modes versus their frequency. The averaging of the modes themselves cannot however be straightforward since a phase shift between them can exist and has to be accounted for, otherwise the modes simply destruct each other. Thus, one of the modes is chosen as the phase reference while the others are phase-shifted, namely by multiplying them by $e^{i\phi}$ with ϕ between 0 and 2π . The best phase shift for each mode is obtained when the correlation between the reference mode and the phase-shifted mode is the highest. The averaging step can then take place as the modes are all in phase.

By averaging modes obtained from different parts of the same data sequence, this technique can reduce the last snapshot bias, provided the computed basis is relevant. However, to successfully apply this method, long data sequences are required in order to be split into different blocks. In addition, the phenomenon is required to remain steady over the observation time.

4. Dynamic analysis

This section aims at (1) comparing the two computation techniques presented in section 2.1 with experimental data and (2) illustrating the kind of information which can be obtained from the computation of multi-variable DMD. Examples are carried out on data from a turbulent test bench featuring a swirled injection of a propane/air premixing. The chamber is equipped with microphones and photo-multipliers synchronized with a time resolved PIV setup. The experiment is deeply presented by Lamraoui *et al.* (2011).

The first computations showed a strong difference on the DMD spectra depending on the decomposition algorithm. Recommendations read in the literature were encouraging to use the \tilde{S} method (Eq. 2.6): "*... a practical implementation [of the S method] yields an ill-conditioned algorithm that is often not capable of extracting more than the first or first two dominant dynamic modes. This is particularly true when the data stem from an experiment...*" (Schmid 2010). The two methods are first used to decompose the velocity field of the swirled flow. Figure 4 presents the two spectra obtained with the two methods. On the top, the \tilde{S} method provides a noisy spectra, the identification of clear dominant peaks is impossible. The reconstruction of spatial modes associated to the highest peaks does not feature coherent structures and the dynamics of the flow cannot be described. The middle subfigure shows the spectrum obtained with the S method. The dominant peak corresponds to the mean flow and a tiny dynamics is observed around 480 Hz. This frequency represents much more the dynamics of the flow clearly controlled by a strong average axial flow and a natural jet instability around 500 Hz. The 482 Hz-mode representation shows the natural instability of the jet where coherent structures can be observed despite the low level of the mode. A deep look at the two spectra shows that the dominant peaks observed with the first method correspond to the most damped modes. Indeed, the way the mode amplitude is computed enforces artificially the damped modes. This bias in the \tilde{S} method forces us to use the most traditional method with the S matrix.

Finally, the multi-variable method is used to decompose the turbulent reactive flow variables. Velocities, pressure and radical emission are decomposed simultaneously, and the spectra of each variable is plotted in figure 5. It allows to show the mechanisms underlying to combustion dynamics. Pressure is strongly marked by the eigenmodes of the test bench. The first two modes correspond to the first two longitudinal modes of the chamber. The second spectrum shows that the velocity field does not feature the same dynamics. At frequencies corresponding to the acoustic modes, the velocity field has no coherent intense structures. The dynamics is contained in a natural mode of the jet which can be observed by reconstructing the corresponding mode. The photomultiplier is sensitive to both the pressure and velocity fluctuations but the coupling mechanisms with heat release are different. The main heat release fluctuations indirectly come from pressure oscillations which have an impact on the injection lines (Lamraoui *et al.* 2011). Another part of the heat release oscillations come directly from the perturbation of the velocity field and so the flame position. Further processing is required to deeply characterize the coupling but DMD already revealed useful information since each mode is associated with one frequency and one damping coefficient, allowing to decompose physically the data fields.

5. Conclusion

The purpose of this study was to explore the different parameters influencing the quality and the precision of the decomposition. It is shown that the choice of the sequence

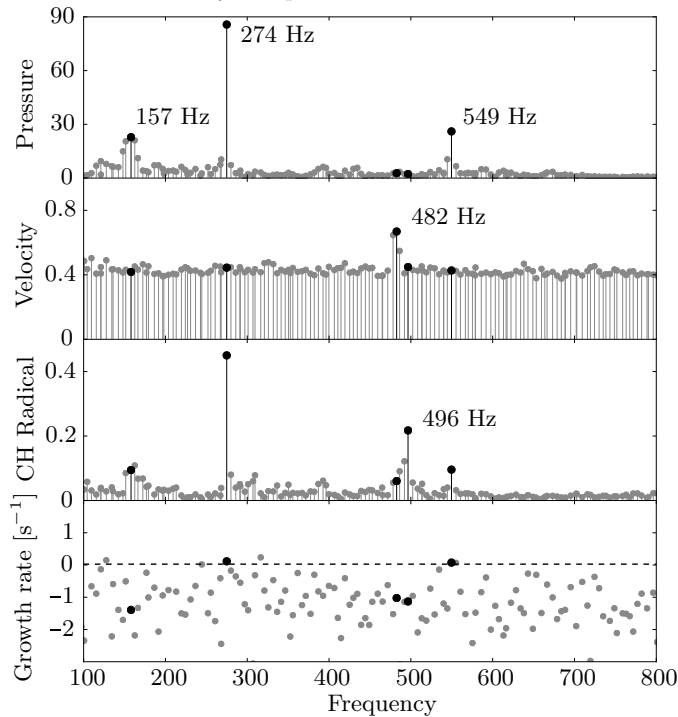


FIGURE 5. The multi-variable DMD allows to plot one spectra for each quantity with a common frequency basis. In a turbulent reactive flow, the dynamic of each variable may be different.

of snapshots among the data series may strongly modify the decomposition and thus the decomposition technique. Finally, the first computations show the great potential of the technique to highlight the dynamical coupling in the reactive turbulent flows.

Acknowledgments

The authors gratefully acknowledge the CTR for the support in this study. The experiments have been conducted with the precious help of researchers in EM2C laboratory: Philippe Scoufflaire, Sébastien Ducruix, Thierry Schuller and the graduate students Ammar Lamraoui and Theodore Providakis.

REFERENCES

- ALDÉN, M., BOOD, J., LI, Z. & RICHTER, M. 2011 Visualization and understanding of combustion processes using spatially and temporally resolved laser diagnostic techniques. *Proc. Comb. Instit.* **33** (1), 69–97.
- BALLESTER, J. & GARCÍA-ARMINGOL, T. 2010 Diagnostic techniques for the monitoring and control of practical flames. *Prog. Ener. Comb. Sci.* **36** (4), 375–411.
- BERKOOZ, G., HOLMES, P. & LUMLEY, J. 1993 The proper orthogonal decomposition in the analysis of turbulent flows. *Annual Review of Fluid Mechanics* **25**, 539–575.
- BORÉE, J. 2003 Extended proper orthogonal decomposition: a tool to analyse correlated events in turbulent flows. *Experiments in Fluids* **35** (2), 188–192.
- CANDEL, S., DUROX, D., DUCRUIX, S., BIRBAUD, A. L., NOIRAY, N. & SCHULLER,

- T. 2009 Flame dynamics and combustion noise: progress and challenges. *Journal of Sound and Vibration* **8** (1), 1–56.
- CHEN, K., TU, J., & ROWLEY, C. 2012 Variants of dynamic mode decomposition: Boundary condition, koopman, and fourier analyses, *Journal of Nonlinear Science*, Online First, doi:10.1007/s00332-012-9130-9.
- DUWIG, C., DUCRUIX, S. & VEYNANTE, D. 2012 Studying the stabilization dynamics of swirling partially premixed flames by proper orthogonal decomposition. *Journal of Engineering for Gas Turbines and Power* **134** (10), 101501.
- DUWIG, C. & IUDICIANI, P. 2010 Extended proper orthogonal decomposition for analysis of unsteady flames. *Flow, Turbulence and Combustion* **84**, 25–47.
- GILLIAM, X., DUNYAK, J. P., SMITH, D. A. & WU, F. 2004 Using projection pursuit and proper orthogonal decomposition to identify independent flow mechanisms. *Journal of Wind Engineering and Industrial Aerodynamics* **92** (1), 53 – 69.
- GLEZER, A., KADIOGLU, Z. & PEARLSTEIN, A. J. 1989 Development of an extended proper orthogonal decomposition and its application to a time periodically forced plane mixing layer. *Physics of Fluids* **1**, 1363–1373.
- HUANG, Y. & YANG, V. 2009 Dynamics and stability of lean-premixed swirl-stabilized combustion. *Progress in Energy and Combustion Science* **35** (4), 293 – 364.
- LAMRAOUI, A., RICHECOEUR, F., SCHULLER, T. & DUCRUIX, S. 2011 A methodology for on the fly acoustic characterization of the feeding line impedances in a turbulent swirled combustor. *Journal of Engineering for Gas Turbines and Power* **133** (1).
- MAUREL, S., BORÉE, J. & LUMLEY, J. L. 2001 Extended proper orthogonal decomposition: Application to jet/vortex interaction, *Flow, Turb. Comb.* **67**(2), 125–136.
- MULD, T. W., EFRAIMSSON, G. & HENNINGSON, D. S. 2012 Flow structures around a high-speed train extracted using proper orthogonal decomposition and dynamic mode decomposition. *Computers & Fluids* **57**, 87–97.
- PROVIDAKIS, T., ZIMMER, L., SCOUFFLAIRE, P. & DUCRUIX, S. 2012 Characterization of the acoustic interactions in a two-stage multi-injection combustor fed with liquid fuel. *Journal of Engineering for Gas Turbines and Power* .
- ROWLEY, C. W., MEZIC, I., SHERVIN, B., PHILIPP, S. & HENNINGSON, D. S. 2009 Spectral analysis of nonlinear flows. *Journal of Fluid Mechanics* **641**, 115–127.
- SCHMID, P. 2011 Application of the dynamic mode decomposition to experimental data. *Experiments in Fluids* **50**, 1123–1130.
- SCHMID, P., LI, L., JUNIPER, M. & PUST, O. 2011 Applications of the dynamic mode decomposition. *Theoretical and Computational Fluid Dynamics* **25**, 249–259.
- SCHMID, P., VIOLATO, D. & SCARANO, F. 2012 Decomposition of time-resolved tomographic piv. *Experiments in Fluids* pp. 1–13.
- SCHMID, P. J. 2010 Dynamic mode decomposition of numerical and experimental data. *Journal of Fluid Mechanics* **656**, 5–28.
- SCHULZ, C. & SICK, V. 2005 Tracer-lif diagnostics: quantitative measurement of fuel concentration, temperature and fuel/air ratio in practical combustion systems. *Progress in Energy and Combustion Science* **31** (1), 75–121.
- SEMERARO, O., BELLANI, G. & LUNDELL, F. 2012 Analysis of time-resolved piv measurements of a confined turbulent jet using pod and koopman modes. *Experiments in Fluids* pp. 1–18.
- STÖHR, M., SADANANDAN, R. & MEIER, W. 2011 Phase-resolved characterization of vortex–flame interaction in a turbulent swirl flame. *Experiments in Fluids* pp. 1–15.